Molecular Therapy
Methods & Clinical Development
Original Article

Transduction Pattern of AAVs in the Trabecular Meshwork and Anterior-Segment Structures in a Rat Model of Ocular Hypertension

Si Hyung Lee,[1,2] Kyeong Sun Sim,[1,2] Chan Yun Kim,[3] and Tae Kwann Park[1,2]

[1]Department of Ophthalmology, College of Medicine, Soonchunhyang University, Cheonan 31151, Republic of Korea; [2]Department of Ophthalmology, Soonchunhyang University Hospital Bucheon, Bucheon 14584, Republic of Korea; [3]Institute of Vision Research, Department of Ophthalmology, Severance Hospital, Yonsei University, College of Medicine, Seoul 03722, Korea

Adeno-associated viruses (AAVs) are the vector of choice for gene therapy in the eye, and self-complementary AAVs (scAAVs), which do not require second-strand DNA synthesis, can be transduced into cells of the trabecular meshwork (TM). The scAAV transduction patterns in the anterior segment of normotensive eyes have been investigated previously, but those in ocular hypertensive (OHT) eyes have not. We assessed the transduction efficiencies of AAV serotypes 2, 5, and 8 in the anterior-segment structures of the eyes of Sprague-Dawley rats with OHT by circumlimbal suturing, followed 3 days later by intracameral injection of scAAV serotype 2 (scAAV2), scAAV5, or scAAV8 packaged with EGFP. The transduction of scAAV2 and scAAV5 in the TM of OHT rats was markedly enhanced after 1 month, and transduction of scAAV5 was more efficient than that of scAAV2; transduction of scAAV8 into the TM did not occur. The transduction of scAAV2, scAAV5, and scAAV8 was enhanced in the ciliary body, iris, and corneal endothelium of the OHT eyes for 3 months. The expression levels of receptors for scAAV2 and scAAV5 were significantly increased in the OHT compared with control eyes. The results demonstrated that scAAV2 and scAAV5 target the ciliary body and TM in OHT eyes, and that the OHT-related changes in anterior-segment structures enhance scAAV transduction.

INTRODUCTION

Glaucoma, a chronic progressive glaucomatous optic neuropathy resulting in visual-field defects, is a leading cause of irreversible blindness worldwide.[1,2] Intraocular pressure (IOP) is an important risk factor for glaucoma, the treatment of which involves lowering the IOP to prevent glaucomatous damage. IOP can be reduced by daily-use eye drops, but the unpleasant complications can reduce patient compliance with glaucoma treatment. In patients with uncontrolled refractory glaucoma, filtering or tube surgeries are performed, but this can lead to sight-threatening complications, e.g., postoperative hypotony,[3,4] suprachoroidal hemorrhage,[5–7] blebitis, and endophthalmitis.[8] Therefore, ocular gene therapy may be a useful strategy for glaucoma, and patients may benefit from the prolonged effect of a single dose.

Adeno-associated viruses (AAVs) are the vector of choice for ocular gene therapy due to their safety and ability to transfer genes into various ocular cells, including those of the retina. Based on the efficacy of AAV-based gene therapy against Leber's congenital amaurosis,[9–11] preclinical and clinical studies of AAV-based gene therapy for retinal diseases are underway.[12–16] Whereas transduction of AAVs into the outer and inner retina following subretinal or intravitreal administration, respectively, is well-established, few studies have investigated the ability of AAVs to target the outflow tract, particularly the trabecular meshwork (TM) and other anterior-segment structures. AAV targeting of these tissues may be important for the treatment of glaucoma.

Transduction of AAVs into the TM is reportedly limited by down-regulation of host DNA replication, preventing conversion of the single-stranded AAV genome into double-stranded DNA.[17–19] To overcome this, recent studies have used self-complementary AAVs (scAAVs), most frequently serotype 2 (scAAV2), a second-generation AAV that carries the sense and antisense cDNA strands of the transgene, which showed a high level of transduction in the TM and anterior-segment structures in rodent and simian models.[20–22] However, because patients with ocular hypertension (OHT) may benefit from the enhanced outflow caused by ocular gene therapy targeting the TM, investigation of scAAV transduction efficiency in the TM and other anterior-segment tissues in OHT eyes is a necessary prerequisite for using AAV gene therapy to treat IOP in glaucomatous eyes.

We investigated the transduction patterns of scAAV2, scAAV5, and scAAV8 in the TM and anterior-segment structures of the eyes of rats with OHT. We also examined the expression levels of AAV receptors in the anterior segment.

Received 25 March 2019; accepted 27 June 2019;
https://doi.org/10.1016/j.omtm.2019.06.009.

Correspondence: Tae Kwann Park, MD, PhD, Department of Ophthalmology, Soonchunhyang University Hospital Bucheon, 170 Jomaru-ro, Wonmi-gu, Bucheon 14584, Republic of Korea.
E-mail: tkpark@schmc.ac.kr

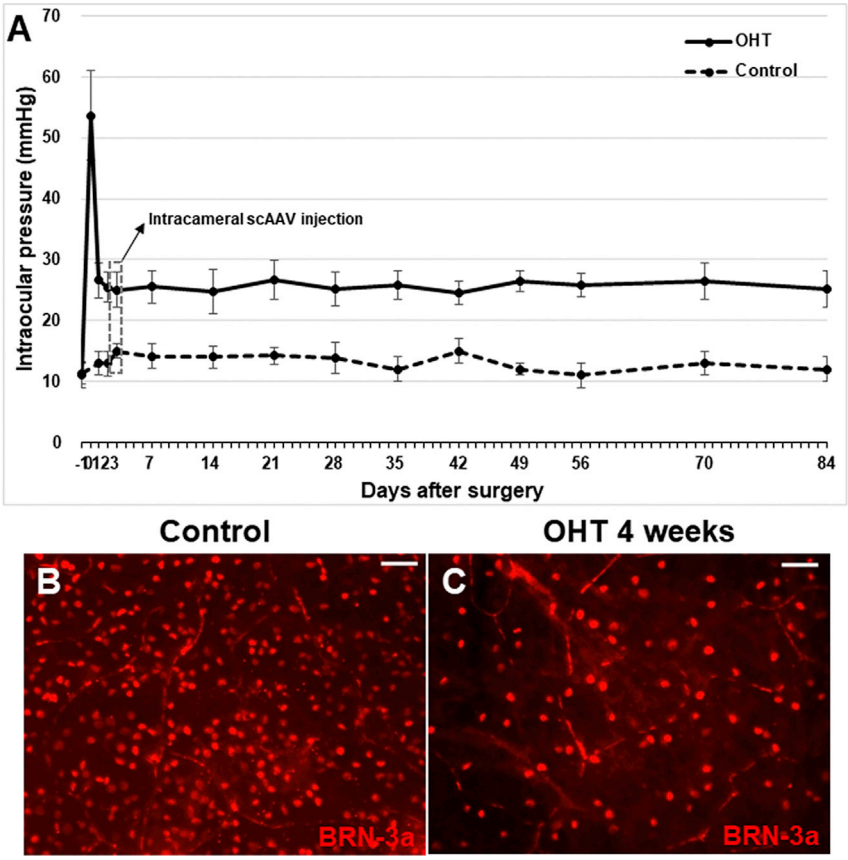

Figure 1. Rat Model of OHT

IOP was significantly elevated from the time immediately after suturing (54 ± 7 mm Hg) until the end of the experiment (control [n = 15], 13 ± 2 mm Hg; OHT [n = 30], 27 ± 3 mm Hg at 3 months) (A). Immunostaining of BRN-3a at 4 weeks revealed a markedly decreased number of RGCs in OHT eyes compared with the control (B and C). Data are means ± SEM. Scale bars, 20 μm. OHT, ocular hypertension.

RESULTS

IOP Was Elevated and the Number of Retinal Ganglion Cells (RGCs) Was Decreased in OHT Eyes

IOP increased significantly (54 ± 7 mm Hg) immediately after circumlimbal suturing and then decreased to 27 ± 3 mm Hg after 24 h. IOP in OHT eyes remained significantly higher (25 ± 3 mm Hg) compared with the control at 3 months ($p < 0.001$) (Figure 1A). IOP of control eyes was 12 ± 2 mm Hg at baseline and 13 ± 2 mm Hg at the end of the experiment. To verify the OHT model, we examined the number of RGCs in retinal whole mounts. At 4 weeks, the number of RGCs expressing BRN-3a was markedly decreased in OHT compared with control eyes (Figure 1B).

Transduction Patterns of scAAV2, scAAV5, and scAAV8 in the Anterior Segment

In control eyes without vector injection, EGFP expression was not detectable in the TM and parts of the ciliary body (Figures 2A and 2E), whereas EGFP expression was minimal after scAAV2 (Figures 2B and 2F) and scAAV5 transduction (Figures 2C and 2G) and absent after scAAV8 transduction (Figures 2D and 2H). In contrast, in OHT eyes, EGFP expression in the TM and ciliary body was markedly increased after scAAV2 and scAAV5 transduction. Transduction of scAAV2 was enhanced to a greater degree in the ciliary body than in the TM (Figures 2J and 2N), whereas transduction of scAAV5 was greatest in the TM and Schlemm's canal (Figures 2K and 2O). Transduction of scAAV8 was detected in the ciliary body, but not the TM, of OHT eyes (Figures 2L and 2P). In OHT eyes without vector administration, no EGFP expression was visible (Figures 2I and 2M).

Cross-sectional images of the iris and cornea of control eyes without vector injection showed no signs of transduction, while scarce EGFP expression on the posterior surface of the iris and corneal endothelium was visible in eyes with vector administration (Figures 3A–3C and 3G–3I). However, transduction of the three serotypes was markedly increased in the iris and corneal endothelium of OHT eyes (Figures 3D–3F and 3J–3L).

The increased expression of EGFP in OHT eyes persisted until 3 months after vector injection. The transduction patterns at 3 months were similar to those at 1 month after vector administration; scAAV2 showed marked localization in the ciliary body and TM (Figure 4A), whereas scAAV5 was more localized in the TM and Schlemm's canal (Figure 4B). At 1 month after vector injection, scAAV8 was localized in the ciliary body (Figure 4C). At 3 months after vector administration, the transduction patterns of the three scAAV serotypes in the iris and corneal endothelium of OHT eyes were consistent with those at 1 month after vector injection (Figures 4D–4I).

Expression of AAV Receptors in OHT Eyes

The efficiency of vector transduction is influenced by receptor-mediated AAV attachment.[23] We next performed immunohistochemical analysis of receptors for AAV2 (perlecan and syndecan), AAV5 (2, 3-linked sialic acid), and AAV8 (67-kDa laminin receptor). The expression of perlecan, also known as heparin sulfate proteoglycan (HSPG)-2, was increased in the ciliary body, TM, iris surface, and corneal endothelium of OHT eyes (Figures 5A–5F). The expression levels of syndecan in the TM, ciliary body, and corneal endothelium of OHT eyes were similar to those of perlecan (Figures 5G, 5I, 5J, and 5L), whereas syndecan expression was increased on the iris surface of OHT eyes (Figures 5H and 5K). Expression of the 67-kDa laminin receptor was markedly enhanced in the ciliary body, iris, and corneal endothelium, yet similar in the TM, in OHT compared with control

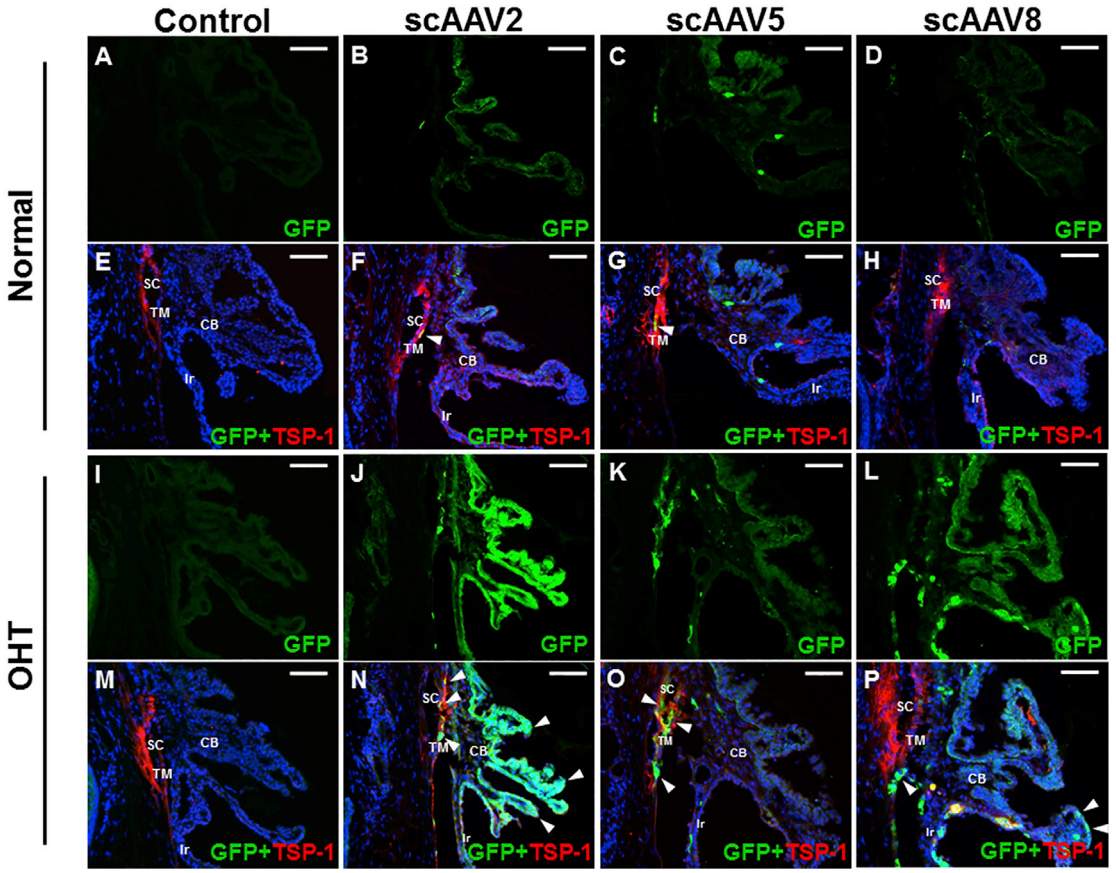

Figure 2. scAAV Transduction Patterns in the TM and Ciliary Body of OHT and Control Eyes

In vector uninjected eyes, EGFP expression was not detected in both normotensive (A and E) and OHT (I and M) eyes. In control eyes with vector injection, EGFP expression in the TM and parts of the ciliary body was scarce after scAAV2 (B and F) and scAAV5 (C and G) transduction and absent after scAAV8 transduction (D and H). In OHT eyes, EGFP expression in the TM and ciliary body was markedly increased after scAAV2 (J and N) and scAAV5 (K and O) transduction. Specifically, in OHT eyes, scAAV2 transduction was localized in both the TM and ciliary body, whereas scAAV5 transduction was localized in the TM and Schlemm's canal; however, scAAV8 transduction was not observed in the TM but was high in the ciliary body (L and P). Images are representatives of 45 mice analyzed (30 for OHT group and 15 for control). Scale bars, 20 μm.

eyes (Figures 6A–6F). Immunostaining of Maakia Amurensis Lectin II (MAL II), which selectively binds to α-2,3 linked sialic acid, revealed that expression of 2,3-linked sialic acid was upregulated in the TM, ciliary body, iris, and corneal endothelium of OHT eyes (Figures 6G–6L). Sites with upregulated AAV receptor expression, including perlecan, syndecan, 2,3-linked sialic acid, and 67-kDa laminin receptor, demonstrated co-localization with GFP expression (Figure S1), supporting that upregulated receptor expression may partially contribute to the enhanced scAAV transduction in anterior-segment tissues of OHT eyes.

According to qRT-PCR, mRNA levels of the AAV receptors were significantly enhanced in the anterior segment of OHT compared with control eyes (Figure 6M).

DISCUSSION

Current treatment regimens for glaucoma, although effective in most cases, have unwanted side effects or complications, and so new therapeutic modalities are needed. AAV-based gene therapy has been demonstrated to be safe and effective against various retinal diseases, and a single dose exerts a long-term therapeutic effect. However, few studies have evaluated AAV-based gene therapy for glaucoma, and the transduction patterns in the anterior-segment structures of OHT eyes are unknown. In this study, transduction of scAAV2, scAAV5, and scAAV8 was enhanced in the eyes of OHT rats compared with control rats for 3 months. Moreover, the transduction patterns differed among the three scAAV serotypes; transduction was greatest in the ciliary body and TM for scAAV2, compared with the TM and Schlemm's canal for scAAV5. In addition, the expression of AAV receptors was increased in the anterior-segment tissues of OHT eyes.

The transduction patterns of a variety of AAV serotypes in the anterior-segment tissues of non-OHT eyes have been investigated. Similar to our findings, scAAV2, the AAV serotype most frequently used for ocular gene therapy, showed transduction in the TM,

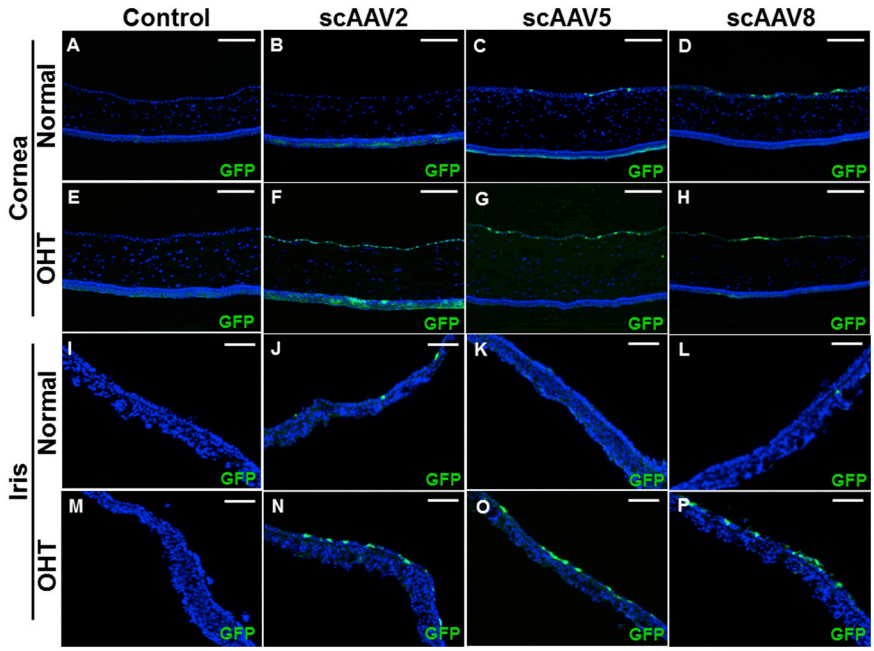

Figure 3. Cross-Sectional Images of the Corneal Endothelium and Iris of Control and OHT Eyes Administered scAAV2, scAAV5, or scAAV8

No EGFP expression was detectable in both normotensive (A and E) and OHT, vector uninjected (I and M) eyes. EGFP expression was scarce on the posterior surface of the iris and corneal endothelium of control eyes administered scAAV2 (B and F), scAAV5 (C and G), and scAAV8 (D and H). Transduction of scAAV2 (J and N), scAAV5 (K and O), and scAAV8 (L and P) was markedly increased in the iris and corneal endothelium of OHT eyes. Pictures are representatives of 45 mice analyzed (30 for OHT group and 15 for control). Scale bars, 20 μm.

ciliary body, iris, and corneal endothelium of live animals without inducing an inflammatory response.[20,22,24] Buie et al.[20] reported that intracameral injection of scAAV2-GFP resulted in persistent gene expression in the TM for more than 2 years. Also, transduction of scAAV2 has been demonstrated in primary human TM and porcine-perfused organ cultures.[25] Intracameral injection of scAAV5 in live rats resulted in greater transduction in the TM than did scAAV2.[25] Furthermore, the magnitude of scAAV5 transduction in the TM and Schlemm's canal was greater than that of the other serotypes. In contrast, in cultured human and porcine TM cells, the transduction efficiency of scAAV5 was greater than that of scAAV2; thus, scAAV tropism may differ among species.[25] However, no study has evaluated recombinant AAV8 or scAAV8 transduction in anterior-segment structures. Overall, the results of prior studies emphasize the importance of selecting the appropriate vector serotype for preclinical studies targeting the TM and anterior-segment tissues.

In this study, transgene expression was greater in OHT eyes than in non-OHT control eyes. Although the transduction patterns of AAV serotypes in normotensive eyes of animals have been investigated, those in OHT eyes were unknown. Moreover, the two previous studies that evaluated the ability of AAV-based gene therapy to lower the IOP in animal models of glaucoma used scAAV2.[21,24] In this study, transduction of scAAV5 was greatest in the TM and Schlemm's canal, whereas that of scAAV2 was greatest in the ciliary body. Therefore, scAAV5 may reduce IOP by targeting the outflow pathway, whereas scAAV2 may lower IOP by reducing aqueous humor production. Thus, AAV-based gene therapy could reduce IOP by enhancing outflow or decreasing aqueous humor production.

The enhanced scAAV transduction in OHT eyes may be caused by upregulation of AAV receptors. HSPGs associated with the cell membrane or extracellular matrix interact with the capsid protein of AAV2 early during transduction.[26,27] Perlecans, which are extracellular matrix-associated HSPGs, facilitate cell entry of the viral capsid by concentrating AAV2 near receptors.[28] Syndecans and glypicans, which are cell membrane-associated HSPGs, are primary receptors for scAAVs that facilitate their interaction with AAV2 co-receptors.[29] In addition, laminins are primary receptors for AAV8,[30] and α-2,3-linked sialic acid is an essential component of the AAV5 receptor complex.[31] Immunohistochemical and qRT-PCR analyses showed that expression level of the receptors for AAV2, AAV5, and AAV8 were increased in the anterior segment of OHT eyes, which may in part explain their enhanced vector transduction. However, there are other previously described primary and secondary receptors for AAV2, AAV5, and AAV8 that were not investigated in this study,[32] and this should be further investigated in future studies. Alternatively, the reduced aqueous outflow may have increased the duration of contact between the viral vector and anterior-segment tissues, which should also be clarified in future investigation.

We performed circumlimbal suturing to increase IOP in rats with OHT.[33–35] This model of OHT is based on ocular compression-mediated suppression of aqueous outflow, but the pattern of IOP elevation is reminiscent of that in acute rather than chronic glaucoma. Therefore, the scAAV transduction patterns in other *in vivo* models of glaucoma with chronic IOP elevation (e.g., the perilimbal and episcleral vein laser coagulation model,[36–38] episcleral vein cauterization model,[39–41] steroid-induced OHT model,[42–45] and TM degenerative model using transgenic animals[46–50]) should also be investigated.

In summary, scAAV transduction was markedly enhanced in OHT compared with non-OHT control eyes, and scAAV2 and scAAV5 targeted the ciliary body and TM, respectively. Therefore, scAAV-based

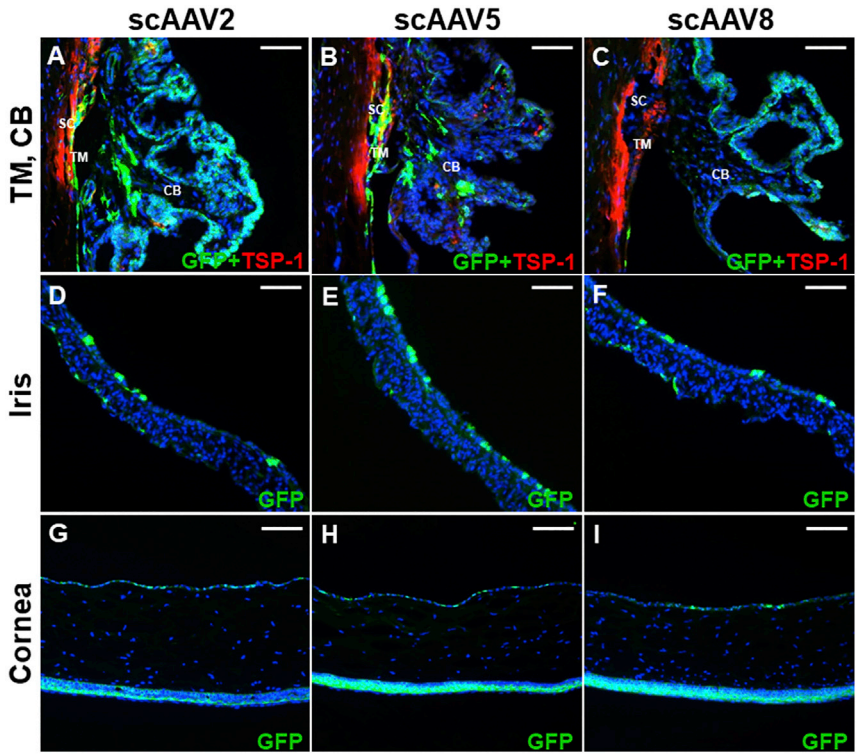

Figure 4. Cross-Sectional Images of the TM, Ciliary Body, Iris, and Corneal Endothelium of OHT and Control Eyes Immunostained for GFP (Green) and TSP-1 (Red) at 3 Months after Circumlimbal Suture

Increased expression of EGFP persisted in OHT eyes until 3 months after suturing. Transduction of scAAV2 was enhanced in the TM and ciliary body (A), and that of scAAV5 in the TM and Schlemm's canal (B) of OHT eyes, similar to the findings at 1 month. Transduction of scAAV8 was enhanced only in the ciliary body, similar to that at 1 month (C). Transduction of scAAV2 (D and G), scAAV5 (E and H), and scAAV8 (F and I) was enhanced in the iris and corneal endothelium. Images are representatives of 45 mice analyzed (30 for OHT group and 15 for control). Scale bars, 20 μm.

gene therapy has potential for treatment of glaucoma. Several genes can be targeted to increase TM outflow or decrease aqueous humor production. Thus, selection of the scAAV serotype appropriate for the target tissue will enable reduction of the IOP of glaucomatous eyes.

MATERIALS AND METHODS

Animals

Forty-five male Sprague-Dawley rats, aged 7–8 weeks (Orient Bio, Sungnam, Republic of Korea), were used in this study. The rats were reared under standard conditions and a 12/12-h light/dark cycle. The care and use of the rats were in compliance with the Association for Research in Vision and Ophthalmology Statement for the Use of Animals in Ophthalmic and Vision Research and were overseen by the Institutional Animal Care and Use Committee of Soonchunhyang University Hospital, Bucheon, Republic of Korea. The rats were sedated by intraperitoneal injection of a mixture of 40 mg/kg zolazepam and tiletamine (Zoletil; Virbac, Carros Cedex, France) and 5 mg/kg xylazine (Rompun; Bayer Healthcare, Leverkusen, Germany).

Rat Model of OHT

Baseline IOP was measured on 2 consecutive days in awake rats using a rebound tonometer (TonoLab; iCare, Helsinki, Finland). To exclude the effect of diurnal IOP fluctuations, we measured IOP between 11 a.m. and 12 p.m. The rats were divided into the OHT (n = 20) and non-OHT control (n = 10) groups. In the rats in the OHT group, circumlimbal suturing was performed to induce IOP elevation in one eye. In brief, circumferential suturing around the globe at approximately 1.0–1.5 mm behind the limbus was performed using 7/0 nylon to pressurize the eyeball (Figure S2). The contralateral eye was untreated. The IOP was measured using a rebound tonometer immediately and at 1, 2, 3, 7, 14, 21, 28, 35, 42, 49, 56, 70, and 86 days after suturing. The IOP was measured in awake animals without topical anesthesia, except for the measurement immediately after circumlimbal suturing, which was performed during recovery from sedation.

Intracameral Administration of scAAVs

At 3 days following circumlimbal suturing, intracameral scAAV injection was performed in the right eye under anesthesia. The rats were anesthetized and placed under a surgical microscope in a slightly lateral position to visualize the eye. After topical anesthesia with one drop of 0.5% proparacaine hydrochloride (Tropherine Eye Drops; Hanmi Pharm, Seoul, Republic of Korea), the cornea was carefully punctured at the limbus using a 30G needle with the bevel pointed upward to prevent contact with the iris or lens. Next, approximately 200 nL of air was slowly injected into the anterior chamber, and the needle was gently removed after checking that no air bubbles had formed. Next, the vector or vehicle control was administered intracamerally using a NanoFil syringe with a blunt 35G needle (World Precision Instruments, Sarasota, FL, USA) through the same corneal puncture, and the position of the needle was maintained for 30 s before removal. Care was taken to maintain the air bubble at the puncture site and not to collapse the anterior chamber when removing the needle. Next, 2 μL scAAV2-EGFP, scAAV5-EGFP, or scAAV8-EGFP (1.0×10^{10} ng/mL; CdmoGen, Cheongju, Republic of Korea) or vehicle control (2 μL balanced salt solution) was injected. Ten rats in the OHT group and five in the control group were subjected to intracameral injection of each AAV serotype.

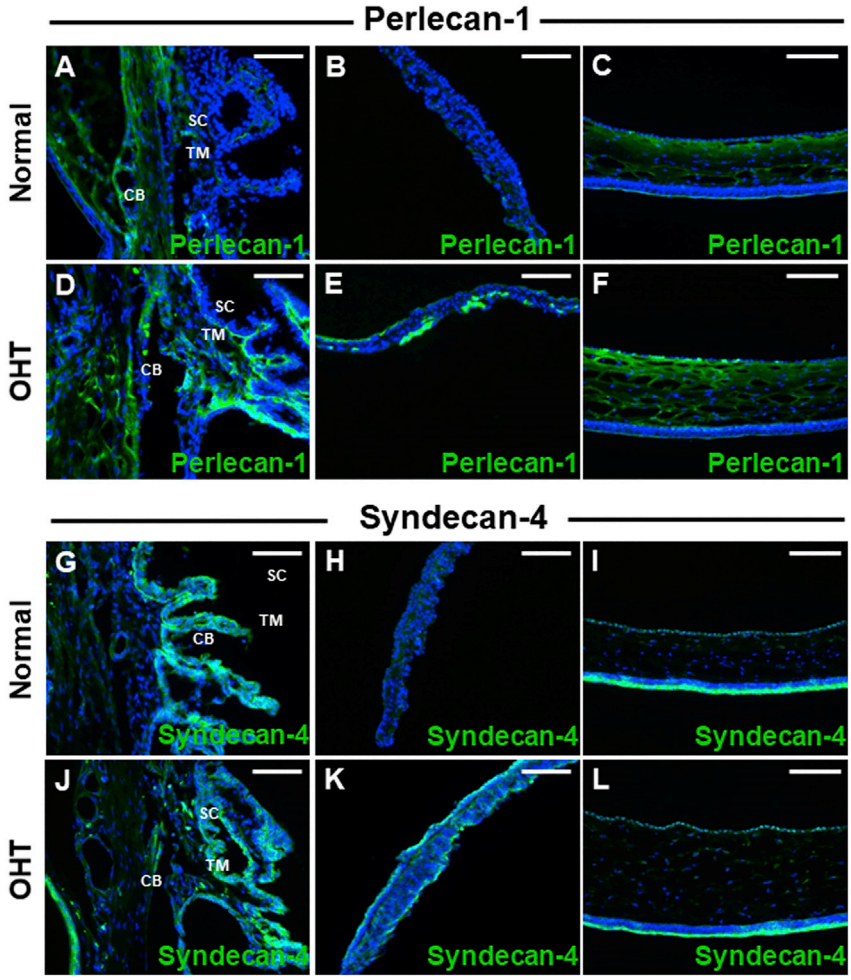

Figure 5. Perlecan-1 and Syndecan-4 Expression in Anterior-Segment Tissues

(A–F) Expression of perlecan-1, an AAV2 receptor, was low in the TM and ciliary body (A), iris (B), and corneal endothelium (C) of control eyes but was increased in the TM and ciliary body (D), iris (E), and corneal endothelium (F) of OHT eyes. (G–L) The expression pattern of the AAV2 receptor syndecan-4 in the TM, ciliary body, and corneal endothelium was similar between OHT (J and L) and control (G and I) eyes but was increased on the iris surface of OHT eyes (H and K). Images are representatives of 45 mice analyzed (30 for OHT group and 15 for control). Scale bars, 20 μm.

Tissue Processing

Tissues were processed for immunohistochemistry as described previously.[51,52] In brief, at 1 and 3 months after AAV administration, the rats were deeply anesthetized and intracardially perfused with 0.1 M PBS containing 150 U/mL heparin, followed by 4% paraformaldehyde (PFA) in 0.1 M PBS. Next, the eyes were enucleated, and a 360-degree sclerotomy just behind the limbus was performed to separate the lens and posterior segment from the anterior segment. Tissues were fixed in 4% PFA, incubated in 30% sucrose in PBS overnight, and embedded in Optimal Cutting Temperature compound. Serial 10-μm sections were cut and mounted on adhesive microscope slides (Histobond; Marienfeld-Superior, Lauda-Königshofen, Germany). For retinal whole mounts, OHT and non-OHT eyes were dissected into posterior eyecups and fixed in 4% PFA, and flattened retinal whole mounts were prepared by making four equidistant cuts.

Immunohistochemistry

Transverse sections of anterior-segment tissue were blocked in 0.1% Triton X-100 in 5% goat serum for 1 h and incubated overnight at 4°C with the primary antibodies listed in Table S1. EGFP expression was visualized using an anti-GFP antibody (1:200, ab6556; Abcam, Cambridge, UK). The samples were washed with 0.1 M PBS and incubated with the following secondary antibodies: Alexa Fluor 488-conjugated donkey anti-rabbit immunoglobulin G (IgG; Invitrogen, Carlsbad, CA, USA) and Alexa Fluor 568-conjugated donkey anti-mouse IgG (Invitrogen) for 1 h at room temperature. Nuclei were visualized by staining with DAPI (0.1 mg/mL; Sigma-Aldrich, St. Louis, MO, USA) for 3 min. Retinal whole mounts were stained as above, with the exception of DAPI. For MAL II immunohistochemistry (1:200, B-1265; Vector Laboratories, Burlingame, CA, USA), samples were incubated at room temperature for 2 h without a secondary antibody. All samples were examined and photographed using an Axioplan microscope at ×200 magnification (Carl Zeiss, Oberkochen, Germany) and a 1,500-ms exposure. Images of the TM, ciliary body, iris, and corneal endothelium were obtained using a monochromatic charge-coupled device camera (Axio-CamMRm; Carl Zeiss) and AxioVision image-capture software (Carl Zeiss). Images of the peripheral (three images), middle (two images), and central (two images) regions of retinal whole mounts were obtained for enumeration of RGCs.

qRT-PCR

The eyeball of deeply anesthetized rats was enucleated, and the lens and posterior segment (including the retina, choroid, and sclera) were removed. Total RNA was extracted from the anterior segment (cornea, iris, ciliary body, and TM) using TRIzol reagent (Invitrogen, Tokyo, Japan). RNA (2 μg) was reverse-transcribed into cDNA using Superscript III (Invitrogen), and PCR amplification was performed using SYBR Green (Invitrogen) and the primers listed in Table S2. The $2^{-\Delta\Delta Ct}$ method was used to determine the fold changes in mRNA levels, which were normalized to that of *GAPDH*. The experiment was conducted in triplicate.

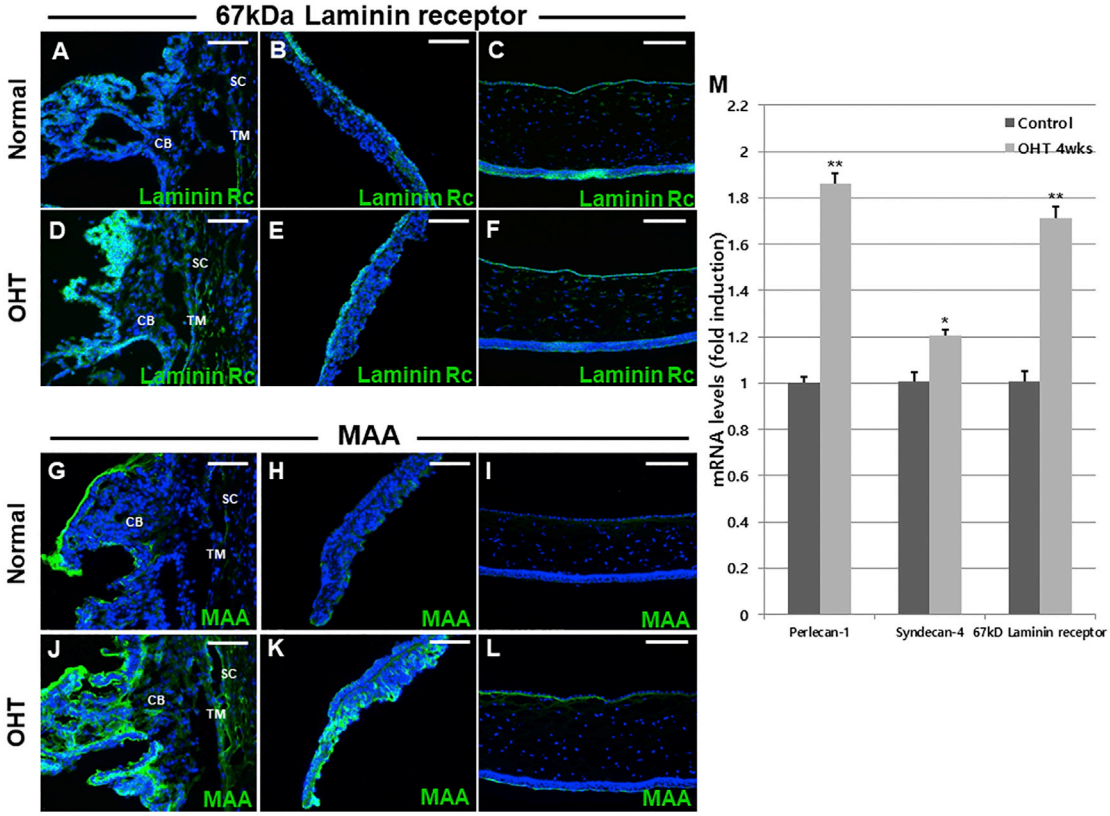

Figure 6. Expression of 67-kDa Laminin Receptor and 2,3-Linked Sialic Acid, and mRNA Levels of scAAV Receptors, in the Control and OHT Eyes

(A–F) Expression of 67-kDa laminin receptor, a receptor for AAV8, was markedly enhanced in the ciliary body (A), iris (B), and corneal endothelium (C) of OHT compared with control eyes (D–F) but was similar in the TM between OHT and control eyes (A and D). Immunostaining with MAL II revealed upregulated expression of 2,3-linked sialic acid in the TM, ciliary body (G and J), iris (H and K), and corneal endothelium (I and L) of OHT eyes (G–L). qRT-PCR analysis showed that the mRNA levels of perlecan-1, syndecan-4, and 67-kDa laminin receptor were significantly elevated in the anterior segment of OHT compared with control eyes (M). Immunohistochemistry images are representatives of 45 mice analyzed (30 for OHT group and 15 for control). Scale bars, 20 μm. Data are means ± SEM.

Statistical Analysis

Data are expressed as means ± SE and were compared by Student's t test. Statistical analyses were conducted using SPSS for Windows software (version 20.0; SPSS, Chicago, IL, USA). A p value <0.05 was taken to indicate statistical significance.

SUPPLEMENTAL INFORMATION

Supplemental Information can be found online at https://doi.org/10.1016/j.omtm.2019.06.009.

AUTHOR CONTRIBUTIONS

Conceptualization, S.H.L. and T.K.P.; Methodology, T.K.P. and S.H.L.; Validation, C.Y.K. and T.K.P.; Investigation, S.H.L. and K.S.S.; Resources, S.H.L. and T.K.P.; Writing – Original Draft, S.H.L.; Writing – Review & Editing, T.K.P. and S.H.L.; Visualization, S.H.L. and C.Y.K.; Supervision, C.Y.K. and T.K.P.; Project Administration, T.K.P.; Funding Acquisition, S.H.L. and T.K.P.

CONFLICTS OF INTEREST

The authors declare no competing interests.

ACKNOWLEDGMENTS

This research was supported by the Basic Science Research Program through the National Research Foundation of Korea (NRF) funded by the Ministry of Education (grant number 2017R1D1A1B03029944) and was partially supported by the Soonchunhyang University research fund.

REFERENCES

1. Resnikoff, S., Pascolini, D., Etya'ale, D., Kocur, I., Pararajasegaram, R., Pokharel, G.P., and Mariotti, S.P. (2004). Global data on visual impairment in the year 2002. Bull. World Health Organ. *82*, 844–851.

2. Quigley, H.A., and Broman, A.T. (2006). The number of people with glaucoma worldwide in 2010 and 2020. Br. J. Ophthalmol. *90*, 262–267.

3. Zacharia, P.T., Deppermann, S.R., and Schuman, J.S. (1993). Ocular hypotony after trabeculectomy with mitomycin C. Am. J. Ophthalmol. *116*, 314–326.

4. Costa, V.P., and Arcieri, E.S. (2007). Hypotony maculopathy. Acta Ophthalmol. Scand. *85*, 586–597.

5. Coleman, A.L., Hill, R., Wilson, M.R., Choplin, N., Kotas-Neumann, R., Tam, M., Bacharach, J., and Panek, W.C. (1995). Initial clinical experience with the Ahmed Glaucoma Valve implant. Am. J. Ophthalmol. *120*, 23–31.

6. Learned, D., and Eliott, D. (2018). Management of Delayed Suprachoroidal Hemorrhage after Glaucoma Surgery. Semin. Ophthalmol. *33*, 59–63.

7. Tuli, S.S., WuDunn, D., Ciulla, T.A., and Cantor, L.B. (2001). Delayed suprachoroidal hemorrhage after glaucoma filtration procedures. Ophthalmology *108*, 1808–1811.

8. Razeghinejad, M.R., Havens, S.J., and Katz, L.J. (2017). Trabeculectomy bleb-associated infections. Surv. Ophthalmol. *62*, 591–610.

9. Bainbridge, J.W., Smith, A.J., Barker, S.S., Robbie, S., Henderson, R., Balaggan, K., Viswanathan, A., Holder, G.E., Stockman, A., Tyler, N., et al. (2008). Effect of gene therapy on visual function in Leber's congenital amaurosis. N. Engl. J. Med. *358*, 2231–2239.

10. Hauswirth, W.W., Aleman, T.S., Kaushal, S., Cideciyan, A.V., Schwartz, S.B., Wang, L., Conlon, T.J., Boye, S.L., Flotte, T.R., Byrne, B.J., and Jacobson, S.G. (2008). Treatment of leber congenital amaurosis due to RPE65 mutations by ocular subretinal injection of adeno-associated virus gene vector: short-term results of a phase I trial. Hum. Gene Ther. *19*, 979–990.

11. Maguire, A.M., Simonelli, F., Pierce, E.A., Pugh, E.N., Jr., Mingozzi, F., Bennicelli, J., Banfi, S., Marshall, K.A., Testa, F., Surace, E.M., et al. (2008). Safety and efficacy of gene transfer for Leber's congenital amaurosis. N. Engl. J. Med. *358*, 2240–2248.

12. Xu, H., Zhang, L., Gu, L., Lu, L., Gao, G., Li, W., Xu, G., Wang, J., Gao, F., Xu, J.Y., et al. (2014). Subretinal delivery of AAV2-mediated human erythropoietin gene is protective and safe in experimental diabetic retinopathy. Invest. Ophthalmol. Vis. Sci. *55*, 1519–1530.

13. Dominguez, J.M., 2nd, Hu, P., Caballero, S., Moldovan, L., Verma, A., Oudit, G.Y., Li, Q., and Grant, M.B. (2016). Adeno-Associated Virus Overexpression of Angiotensin-Converting Enzyme-2 Reverses Diabetic Retinopathy in Type 1 Diabetes in Mice. Am. J. Pathol. *186*, 1688–1700.

14. Birke, M.T., Lipo, E., Adhi, M., Birke, K., and Kumar-Singh, R. (2014). AAV-mediated expression of human PRELP inhibits complement activation, choroidal neovascularization and deposition of membrane attack complex in mice. Gene Ther. *21*, 507–513.

15. Maclachlan, T.K., Lukason, M., Collins, M., Munger, R., Isenberger, E., Rogers, C., Malatos, S., Dufresne, E., Morris, J., Calcedo, R., et al. (2011). Preclinical safety evaluation of AAV2-sFLT01: a gene therapy for age-related macular degeneration. Mol. Ther. *19*, 326–334.

16. Park, T.K., Lee, S.H., Choi, J.S., Nah, S.K., Kim, H.J., Park, H.Y., Lee, H., Lee, S.H.S., and Park, K. (2017). Adeno-Associated Viral Vector-Mediated mTOR Inhibition by Short Hairpin RNA Suppresses Laser-Induced Choroidal Neovascularization. Mol. Ther. Nucleic Acids *8*, 26–35.

17. Borrás, T. (2003). Recent developments in ocular gene therapy. Exp. Eye Res. *76*, 643–652.

18. Borrás, T., Brandt, C.R., Nickells, R., and Ritch, R. (2002). Gene therapy for glaucoma: treating a multifaceted, chronic disease. Invest. Ophthalmol. Vis. Sci. *43*, 2513–2518.

19. Borrás, T., Xue, W., Choi, V.W., Bartlett, J.S., Li, G., Samulski, R.J., and Chisolm, S.S. (2006). Mechanisms of AAV transduction in glaucoma-associated human trabecular meshwork cells. J. Gene Med. *8*, 589–602.

20. Buie, L.K., Rasmussen, C.A., Porterfield, E.C., Ramgolam, V.S., Choi, V.W., Markovic-Plese, S., Samulski, R.J., Kaufman, P.L., and Borrás, T. (2010). Self-complementary AAV virus (scAAV) safe and long-term gene transfer in the trabecular meshwork of living rats and monkeys. Invest. Ophthalmol. Vis. Sci. *51*, 236–248.

21. Borrás, T., Buie, L.K., and Spiga, M.G. (2016). Inducible scAAV2.GRE.MMP1 lowers IOP long-term in a large animal model for steroid-induced glaucoma gene therapy. Gene Ther. *23*, 438–449.

22. Bogner, B., Boye, S.L., Min, S.H., Peterson, J.J., Ruan, Q., Zhang, Z., Reitsamer, H.A., Hauswirth, W.W., and Boye, S.E. (2015). Capsid Mutated Adeno-Associated Virus Delivered to the Anterior Chamber Results in Efficient Transduction of Trabecular Meshwork in Mouse and Rat. PLoS ONE *10*, e0128759.

23. Schultz, B.R., and Chamberlain, J.S. (2008). Recombinant adeno-associated virus transduction and integration. Mol. Ther. *16*, 1189–1199.

24. Borrás, T., Buie, L.K., Spiga, M.G., and Carabana, J. (2015). Prevention of nocturnal elevation of intraocular pressure by gene transfer of dominant-negative RhoA in rats. JAMA Ophthalmol. *133*, 182–190.

25. Borrás, T. (2017). The Pathway From Genes to Gene Therapy in Glaucoma: A Review of Possibilities for Using Genes as Glaucoma Drugs. Asia Pac. J. Ophthalmol. (Phila.) *6*, 80–93.

26. Boye, S.L., Bennett, A., Scalabrino, M.L., McCullough, K.T., Van Vliet, K., Choudhury, S., Ruan, Q., Peterson, J., Agbandje-McKenna, M., and Boye, S.E. (2016). Impact of Heparan Sulfate Binding on Transduction of Retina by Recombinant Adeno-Associated Virus Vectors. J. Virol. *90*, 4215–4231.

27. Woodard, K.T., Liang, K.J., Bennett, W.C., and Samulski, R.J. (2016). Heparan Sulfate Binding Promotes Accumulation of Intravitreally Delivered Adeno-associated Viral Vectors at the Retina for Enhanced Transduction but Weakly Influences Tropism. J. Virol. *90*, 9878–9888.

28. Vivès, R.R., Lortat-Jacob, H., and Fender, P. (2006). Heparan sulphate proteoglycans and viral vectors : ally or foe? Curr. Gene Ther. *6*, 35–44.

29. Kern, A., Schmidt, K., Leder, C., Müller, O.J., Wobus, C.E., Bettinger, K., Von der Lieth, C.W., King, J.A., and Kleinschmidt, J.A. (2003). Identification of a heparin-binding motif on adeno-associated virus type 2 capsids. J. Virol. *77*, 11072–11081.

30. Akache, B., Grimm, D., Pandey, K., Yant, S.R., Xu, H., and Kay, M.A. (2006). The 37/67-kilodalton laminin receptor is a receptor for adeno-associated virus serotypes 8, 2, 3, and 9. J. Virol. *80*, 9831–9836.

31. Walters, R.W., Yi, S.M., Keshavjee, S., Brown, K.E., Welsh, M.J., Chiorini, J.A., and Zabner, J. (2001). Binding of adeno-associated virus type 5 to 2,3-linked sialic acid is required for gene transfer. J. Biol. Chem. *276*, 20610–20616.

32. Nonnenmacher, M., and Weber, T. (2012). Intracellular transport of recombinant adeno-associated virus vectors. Gene Ther. *19*, 649–658.

33. Liu, H.H., Bui, B.V., Nguyen, C.T., Kezic, J.M., Vingrys, A.J., and He, Z. (2015). Chronic ocular hypertension induced by circumlimbal suture in rats. Invest. Ophthalmol. Vis. Sci. *56*, 2811–2820.

34. Liu, H.H., and Flanagan, J.G. (2017). A Mouse Model of Chronic Ocular Hypertension Induced by Circumlimbal Suture. Invest. Ophthalmol. Vis. Sci. *58*, 353–361.

35. Zhao, D., Nguyen, C.T., Wong, V.H., Lim, J.K., He, Z., Jobling, A.I., Fletcher, E.L., Chinnery, H.R., Vingrys, A.J., and Bui, B.V. (2017). Characterization of the Circumlimbal Suture Model of Chronic IOP Elevation in Mice and Assessment of Changes in Gene Expression of Stretch Sensitive Channels. Front. Neurosci. *11*, 41.

36. Salinas-Navarro, M., Alarcón-Martínez, L., Valiente-Soriano, F.J., Jiménez-López, M., Mayor-Torroglosa, S., Avilés-Trigueros, M., Villegas-Pérez, M.P., and Vidal-Sanz, M. (2010). Ocular hypertension impairs optic nerve axonal transport leading to progressive retinal ganglion cell degeneration. Exp. Eye Res. *90*, 168–183.

37. Levkovitch-Verbin, H., Quigley, H.A., Martin, K.R., Valenta, D., Baumrind, L.A., and Pease, M.E. (2002). Translimbal laser photocoagulation to the trabecular meshwork as a model of glaucoma in rats. Invest. Ophthalmol. Vis. Sci. *43*, 402–410.

38. Li, R.S., Tay, D.K., Chan, H.H., and So, K.F. (2006). Changes of retinal functions following the induction of ocular hypertension in rats using argon laser photocoagulation. Clin. Exp. Ophthalmol. *34*, 575–583.

39. Ruiz-Ederra, J., and Verkman, A.S. (2006). Mouse model of sustained elevation in intraocular pressure produced by episcleral vein occlusion. Exp. Eye Res. *82*, 879–884.

40. Grozdanic, S.D., Betts, D.M., Sakaguchi, D.S., Kwon, Y.H., Kardon, R.H., and Sonea, I.M. (2003). Temporary elevation of the intraocular pressure by cauterization of vortex and episcleral veins in rats causes functional deficits in the retina and optic nerve. Exp. Eye Res. *77*, 27–33.

41. Bayer, A.U., Danias, J., Brodie, S., Maag, K.P., Chen, B., Shen, F., Podos, S.M., and Mittag, T.W. (2001). Electroretinographic abnormalities in a rat glaucoma model with chronic elevated intraocular pressure. Exp. Eye Res. *72*, 667–677.

42. Sawaguchi, K., Nakamura, Y., Nakamura, Y., Sakai, H., and Sawaguchi, S. (2005). Myocilin gene expression in the trabecular meshwork of rats in a steroid-induced ocular hypertension model. Ophthalmic Res. *37*, 235–242.

43. Shinzato, M., Yamashiro, Y., Miyara, N., Iwamatsu, A., Takeuchi, K., Umikawa, M., Bayarjargal, M., Kariya, K., and Sawaguchi, S. (2007). Proteomic analysis of the trabecular meshwork of rats in a steroid-induced ocular hypertension model: down-regulation of type I collagen C-propeptides. Ophthalmic Res. *39*, 330–337.

44. Razali, N., Agarwal, R., Agarwal, P., Kapitonova, M.Y., Kannan Kutty, M., Smirnov, A., Salmah Bakar, N., and Ismail, N.M. (2015). Anterior and posterior segment

changes in rat eyes with chronic steroid administration and their responsiveness to antiglaucoma drugs. Eur. J. Pharmacol. *749*, 73–80.

45. Razali, N., Agarwal, R., Agarwal, P., Kumar, S., Tripathy, M., Vasudevan, S., Crowston, J.G., and Ismail, N.M. (2015). Role of adenosine receptors in resveratrol-induced intraocular pressure lowering in rats with steroid-induced ocular hypertension. Clin. Exp. Ophthalmol. *43*, 54–66.

46. Libby, R.T., Smith, R.S., Savinova, O.V., Zabaleta, A., Martin, J.E., Gonzalez, F.J., and John, S.W. (2003). Modification of ocular defects in mouse developmental glaucoma models by tyrosinase. Science *299*, 1578–1581.

47. Mabuchi, F., Lindsey, J.D., Aihara, M., Mackey, M.R., and Weinreb, R.N. (2004). Optic nerve damage in mice with a targeted type I collagen mutation. Invest. Ophthalmol. Vis. Sci. *45*, 1841–1845.

48. Malyukova, I., Lee, H.S., Fariss, R.N., and Tomarev, S.I. (2006). Mutated mouse and human myocilins have similar properties and do not block general secretory pathway. Invest. Ophthalmol. Vis. Sci. *47*, 206–212.

49. Zhou, Y., Grinchuk, O., and Tomarev, S.I. (2008). Transgenic mice expressing the Tyr437His mutant of human myocilin protein develop glaucoma. Invest. Ophthalmol. Vis. Sci. *49*, 1932–1939.

50. Senatorov, V., Malyukova, I., Fariss, R., Wawrousek, E.F., Swaminathan, S., Sharan, S.K., and Tomarev, S. (2006). Expression of mutated mouse myocilin induces open-angle glaucoma in transgenic mice. J. Neurosci. *26*, 11903–11914.

51. Lee, S.H., Kim, Y.S., Nah, S.K., Kim, H.J., Park, H.Y., Yang, J.Y., Park, K., and Park, T.K. (2018). Transduction Patterns of Adeno-associated Viral Vectors in a Laser-Induced Choroidal Neovascularization Mouse Model. Mol. Ther. Methods Clin. Dev. *9*, 90–98.

52. Lee, S.H., Colosi, P., Lee, H., Ohn, Y.H., Kim, S.W., Kwak, H.W., and Park, T.K. (2014). Laser photocoagulation enhances adeno-associated viral vector transduction of mouse retina. Hum. Gene Ther. Methods *25*, 83–91.

OMTM, Volume *14*

Supplemental Information

Transduction Pattern of AAVs in the Trabecular Meshwork and Anterior-Segment Structures in a Rat Model of Ocular Hypertension

Si Hyung Lee, Kyeong Sun Sim, Chan Yun Kim, and Tae Kwann Park

Supplemental Figures

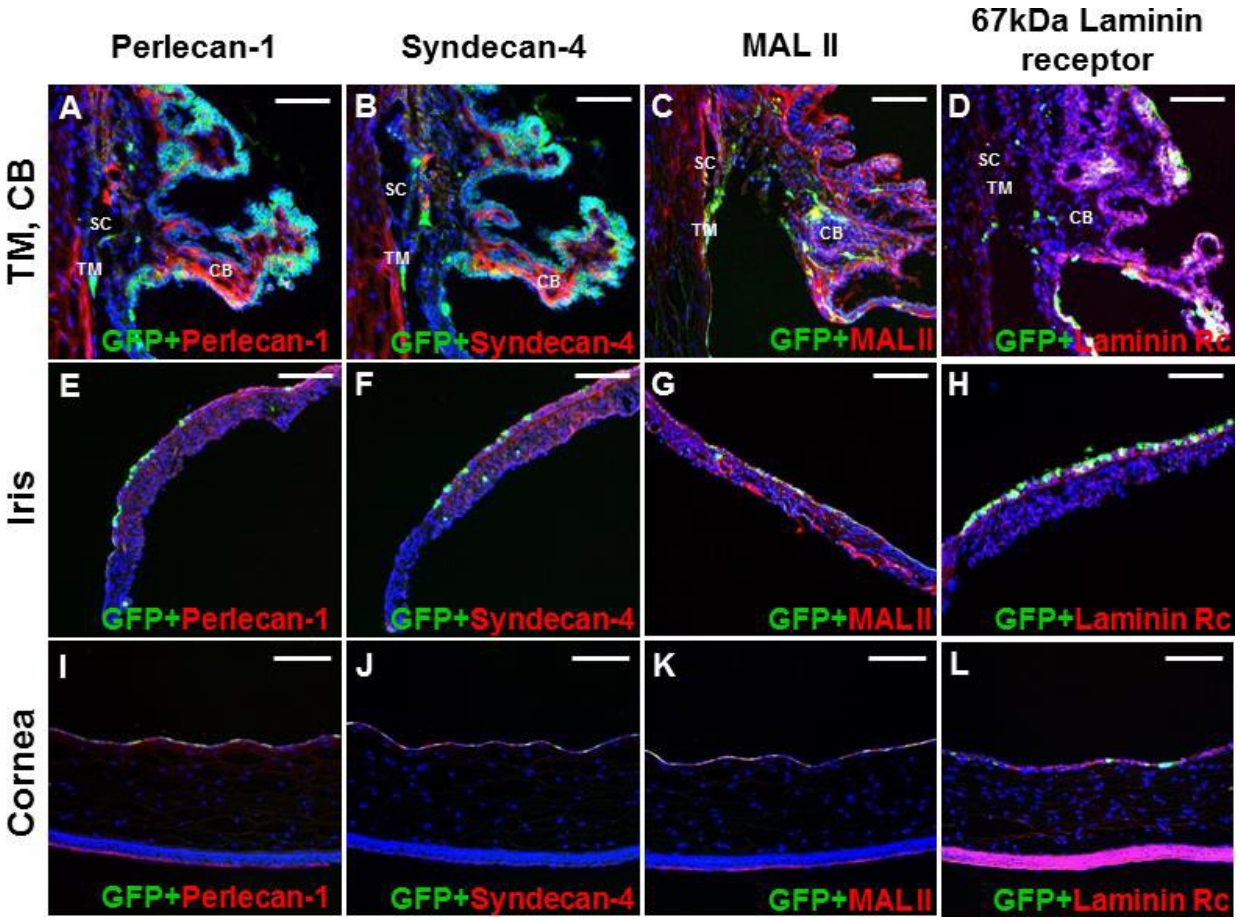

Figure S1. Cross-sectional images of the anterior segment of OHT and control eyes immunostained for GFP (green) and perlecan-1, syndecan-4, MAL II, and 67kDa laminin receptor (red) at 1 months after circumlimbal suture.

Transverse sectional images of anterior segment revealed co-localization of EGFP and receptors for AAV2 (perlecan-1 and syndecan-4), AAV5 (MAL II), and AAV8 (67kDa laminin receptor) in several portion of TM and ciliary body (A-D), iris (E-H), and corneal endothelium (I-L). Images are representatives of 45 mice analyzed (30 for OHT group and 15 for control). Scale bar, 20 μm.

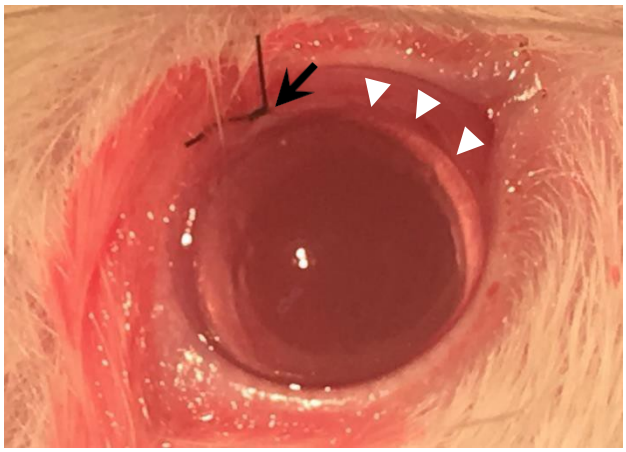

Figure S2. Circumlimbal suture to produce a rat model of OHT.

To produce an OHT rat model, circumlimbal suturing was performed to elevate IOP in one eye. Circumferential suturing around the globe at approximately 1.0–1.5 mm behind the limbus was performed using 7/0 nylon compress and pressurize the eyeball.

Supplemental Tables

Table S1. Primary antibodies used in this study

Target	Host	Manufacturer	Catalog No.	Dilution
GS	Mouse	Millipore, Billerica, MA, USA	MAB302	1:500
CD31	Rat	BD Transduction Laboratories, Lexington, KY, USA	550274	1:100
iba-1	Rabbit	Wako Chemicals, Osaka, Japan	019-19741	1:1000
NeuN	Mouse	Millipore, Billerica, MA, USA	MAB377	1:2000
PKCα	Mouse	Santa Cruz Biotechnology, Dallas, TX, USA	SC-8393	1:1000
Calbindin	Mouse	Sigma-Aldrich, St. Louis, MO, USA	C9848	1:100
Calretinin	Rabbit	Sigma-Aldrich, St. Louis, MO, USA	C7479	1:400
Perlecan	Rat	Invitrogen, Carlsbad, CA, USA	MA5-14641	
Syndecan-4	Rabbit	Abcam, Cambridge, UK	ab24511	1:500
37/67kDa laminin receptor	Rabbit	Abcam Cambridge, UK	ab137388	1:100

Table S2. Primers used in this study

Gene	Primer sequence	
	Forward	**Reverse**
Glypican-1	5'TGGCGCCTACGGTGGAAATGATGT-3'	5'-GAGTGGCGGCCGAGGTCTTCTGTC-3'
Syndecan-4	5'-GAACCATGGCGCCTGTCTGC-3'	5'-CCTGGGCTCCTCCGTGTCATCT-3'
Perlecan-1	5'-AGGTTCCTTTCCCGCCCA-3'	5'-CAACTTGACAGGGATGGCGA-3'
37/67kDa laminin receptor	5'-AGCGAGCTGTGCTGAAGTTT-3'	5'-GTCACCACTAGAAGCCGTGG-3'
GAPDH	5'-ACGGCAAATTCAACGGCA-3'	5'-GGTCATGAGCCCTTCCAC-3'